

AD-A168 012

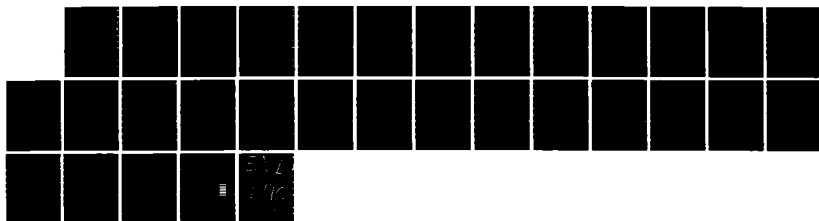
FURTHER RESULTS ON THE INITIATION AND GROWTH OF
ADIABATIC SHEAR BANDS(U) ARMY BALLISTIC RESEARCH LAB
ABERDEEN PROVING GROUND MD T W WRIGHT ET AL. APR 86
BRL-MR-3508

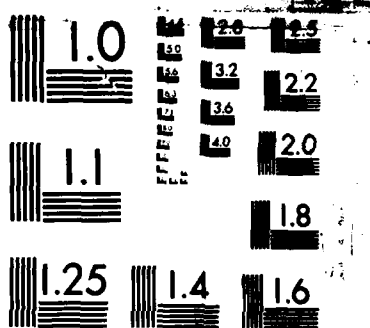
1/1

UNCLASSIFIED

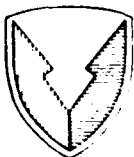
F/G 20/11

NL





MICROCOPY RESOLUTION TEST CHART
NATIONAL BUREAU OF STANDARDS-1963-A



US ARMY
MATERIEL
COMMAND

AD

12

MEMORANDUM REPORT BRL-MR-3508

AD-A168 012

FURTHER RESULTS ON THE
INITIATION AND GROWTH OF
ADIABATIC SHEAR BANDS

Thomas W. Wright
Romesh C. Batra

April 1986

DTIC
SELECTED
MAY 23 1986
A

APPROVED FOR PUBLIC RELEASE; DISTRIBUTION UNLIMITED.

US ARMY BALLISTIC RESEARCH LABORATORY
ABERDEEN PROVING GROUND, MARYLAND

86 5 22 012

Destroy this report when it is no longer needed.
Do not return it to the originator.

Additional copies of this report may be obtained
from the National Technical Information Service,
U. S. Department of Commerce, Springfield, Virginia
22161.

The findings in this report are not to be construed as an official
Department of the Army position, unless so designated by other
authorized documents.

The use of trade names or manufacturers' names in this report
does not constitute indorsement of any commercial product.

UNCLASSIFIED

SECURITY CLASSIFICATION OF THIS PAGE (When Data Entered)

REPORT DOCUMENTATION PAGE		READ INSTRUCTIONS BEFORE COMPLETING FORM
1. REPORT NUMBER Memorandum Report BRL-MR-3508	2. GOVT ACCESSION NO.	3. RECIPIENT'S CATALOG NUMBER
4. TITLE (and Subtitle) Further Results on the Initiation and Growth of Adiabatic Shear Bands		5. TYPE OF REPORT & PERIOD COVERED
		6. PERFORMING ORG. REPORT NUMBER
7. AUTHOR(s) Thomas W. Wright and Romesh C. Batra *		8. CONTRACT OR GRANT NUMBER(s)
9. PERFORMING ORGANIZATION NAME AND ADDRESS USA Ballistic Research Laboratory ATTN: SLCBR-TB Aberdeen Proving Ground, MD 21005-5066		10. PROGRAM ELEMENT, PROJECT, TASK AREA & WORK UNIT NUMBERS 1L161102AH43
11. CONTROLLING OFFICE NAME AND ADDRESS USA Ballistic Research Laboratory ATTN: SLCBR-DD-T Aberdeen Proving Ground, MD 21005-5066		12. REPORT DATE April 1986
		13. NUMBER OF PAGES 28
14. MONITORING AGENCY NAME & ADDRESS (if different from Controlling Office)		15. SECURITY CLASS. (of this report) Unclassified
		15a. DECLASSIFICATION/DOWNGRADING SCHEDULE
16. DISTRIBUTION STATEMENT (of this Report) Approved for public release; distribution is unlimited.		
17. DISTRIBUTION STATEMENT (of the abstract entered in Block 20, if different from Report)		
18. SUPPLEMENTARY NOTES * University of Missouri-Rolla Rolla, Missouri 65401-0249		
19. KEY WORDS (Continue on reverse side if necessary and identify by block number) > Plastic deformation material instability. adiabatic shear bands.		
20. ABSTRACT (Continue on reverse side if necessary and identify by block number) Growth of perturbations in the simple shearing deformation of a softening thermo-visco-plastic solid have been examined by means of a finite element technique. It has been found that very small perturbations grow slowly at first, even though the underlying homogeneous stress-strain response has passed peak stress, but that eventually explosive growth occurs. During the slow growth phase, the stress follows the homogeneous response quite closely, but in the explosive phase, the stress drops precipitously. Large perturbations grow at a larger initial rate, and accelerate rapidly even before peak		

UNCLASSIFIED

SECURITY CLASSIFICATION OF THIS PAGE(When Data Entered)

homogeneous stress. Inclusion of a dipolar plastic effect appears to be stabilizing. Keywords: \rightarrow a fetal (9)

TABLE OF CONTENTS

	<u>Page</u>
LIST OF ILLUSTRATIONS.	5
I. INTRODUCTION AND BASIC EQUATIONS	7
II. HOMOGENEOUS SOLUTIONS AND PERTURBATIONS.	8
III. MODIFICATIONS FOR A DIPOLAR EFFECT	17
IV. DISCUSSION AND CONCLUSIONS	18
REFERENCES	20
DISTRIBUTION LIST.	21

Accession For	
NTIS GRA&I	<input checked="" type="checkbox"/>
DTIC TAB	<input type="checkbox"/>
Unannounced	<input type="checkbox"/>
Justification	
By	
Distribution/	
Availability Codes	
Dist	Avail and/or Special
A-1	



LIST OF ILLUSTRATIONS

<u>FIG. NO.</u>		<u>Page</u>
1	Homogeneous response curves. The reference curve, the isothermal curve for case A, and the adiabatic curves for both cases A and B are shown.	9
2	Temperature perturbations added to the homogeneous response at I.	11
3	Stress vs. average strain (or time, since $\dot{\gamma}_{ave} = 1$). Homogeneous and perturbed responses for cases A and B	12
4	Temperature rise for case A. Upper curves are for the center of the band, lower curves for the edge. Solid curve is the homogeneous case	13
5	Plastic strain rate in the center of the band for case A. Reference rate (homogeneous deformation) is close to 1. . . .	14
6	Cross sections of temperature rise at times indicated	15
7	Cross sections of plastic strain rate at times indicated. . .	16
8	Plastic strain rate in the center of the band for case B at early times. Dipolar material compared to simple material. .	19

I. INTRODUCTION AND BASIC EQUATIONS

Adiabatic shear banding is a localization phenomenon that occurs during high rate plastic deformation in many materials. Since the heat generated by plastic flow usually tends to lower the flow stress, the response curve for adiabatic homogeneous deformation will fall below the isothermal response. If this thermal softening is stronger than both work and rate hardening together, then eventually a peak stress occurs at a critical value of strain, followed by decreasing stress for further increments of strain. Such a situation is generally unstable and presents an opportunity for strain localization to occur. In recent years there has been considerable interest in developing a quantitative, dynamical theory of adiabatic shear banding. Much of the recent literature, as well as some of the pioneering works have been listed and discussed briefly by Clifton, et al.¹ In this paper we present further calculations of the kind given previously by Wright and Batra.² In particular, we show the effect of changing the constitutive rate response and the magnitude of the perturbation. We also examine the effect of adding a gradient or dipolar response to the constitutive equations, at least for early times.

In order to concentrate on fundamentals, consider one-dimensional shearing of a block of material that lies between the boundaries $\bar{y} = \pm h$. The deformation is assumed to be given completely by horizontal shearing. Thus the velocity field may be written

$$\dot{\bar{x}} = \bar{v}(\bar{y}, \bar{t}); \quad \dot{\bar{y}} = 0; \quad \dot{\bar{z}} = 0. \quad (1)$$

As used in Reference 2, the balance and constitutive laws for this case are given here in nondimensional form.

Momentum:	$s_{,y} = \rho \dot{v}$	
Energy:	$\dot{\theta} = k \theta_{,yy} + s \dot{\gamma}_p$	
Elastic Response:	$\dot{s} = \mu (v_{,y} - \dot{\gamma}_p)$	
Reference Plastic Response:	$\kappa = (1 + \frac{\psi}{\psi_0})^n$	(2)
Work Hardening:	$\dot{W}_p = \kappa \dot{\psi} = s \dot{\gamma}_p$	
Yield Surface:	$ s = (1 - a\theta)(1 + b \dot{\gamma}_p)^m \kappa$	

Boundary conditions are $v(\pm 1, t) = \pm 1$, $\theta_{,y}(\pm 1, t) = 0$. In these equations the shear stress is s , mass density is ρ , particle velocity is v , temperature rise is θ , thermal conductivity is k , plastic strain rate is $\dot{\gamma}_p$, shear modulus is μ , work hardening parameter is κ , and plastic strain in a reference test is ψ . The comma denotes partial differentiation with respect to

the spatial coordinate y , and the superimposed dot denotes partial differentiation with respect to time t . In the energy equation plastic working acts as a source term. A linear elastic response is assumed as well as the additive decomposition of shear strain into elastic and plastic parts. The reference plastic response is intended to be simply a curve fit to a slow isothermal test. The work hardening parameter is assumed to depend only on the plastic work no matter what the rate of the test. Finally, the yield surface is taken to depend on plastic strain rate, as well as stress and temperature. When (2)₆ is solved for $\dot{\gamma}_p$ as a function of s , θ , and κ , this last condition is seen to be simply an overstress rule for plastic flow when the stress-temperature point lies outside the static yield surface. The form chosen here is similar to one due to Litonski.³ Note that the thermal softening depends only linearly on temperature.

In Reference 2 the nondimensional variables and parameters are related to their dimensional (barred) counterparts as follows:

$$y = \bar{y}/h \quad t = \bar{t}\dot{\gamma}_0 \quad v = \bar{v}/(h\dot{\gamma}_0) \quad s = \bar{s}/\kappa_0 \quad \theta = (\bar{\theta}\bar{\rho}c_v)/\kappa_0$$

$$\kappa = \bar{\kappa}/\kappa_0 \quad \gamma = \bar{\gamma} \quad \psi = \bar{\psi} \quad \rho = (\bar{\rho}h^2\dot{\gamma}_0^2)/\kappa_0 \quad k = \bar{k}/(\bar{\rho}c_v\dot{\gamma}_0h^2)$$

$$\mu = \bar{\mu}/\kappa_0 \quad a = (\bar{a}\kappa_0)/(\bar{\rho}c_v) \quad b = \bar{b}\dot{\gamma}_0 \quad \dot{\gamma}_p = \dot{\bar{\gamma}}_p/\dot{\gamma}_0$$

where $\dot{\gamma}_0 = \bar{v}(h, \bar{t})/h$ is the average applied strain rate between $\bar{y} = \pm h$, κ_0 is the initial yield stress in the reference test, c_v is the specific heat at constant volume, and \bar{a} , \bar{b} , ψ_0 , m , and n are material constants.

II. HOMOGENEOUS SOLUTIONS AND PERTURBATIONS

If we set $v = y$ and assume that s , θ , and κ are independent of y , then equations (2) reduce to a set of ordinary differential equations in time with s , θ , and κ as dependent variables. For initial conditions we assume $s(0) = 1$, $\theta(0) = 0$, and $\kappa(0) = 1$, so that yielding begins at the initial time. For the assumed visco/plastic flow law, the stress/strain response is a smooth curve, which rises at the elastic slope initially and then, as plastic flow increases and the temperature rises, the curve bends over, passes through a single maximum, and finally decreases with further increments of strain. This type of calculated behavior is well known in the literature, e.g. see References 4, 5, 6, and 7. Figure 1 shows typical results. For curve A, the nondimensional parameters are

$$\rho = 3.928 \times 10^{-5}, \quad k = 3.978 \times 10^{-3}, \quad a = 0.4973, \quad \mu = 240.3$$

$$n = 0.09, \quad \psi_0 = 0.017, \quad b = 5 \times 10^6, \quad m = 0.025$$

and for curve B all the numbers are the same except $b = 5 \times 10^5$ and $m = 0.02$. Also shown in the figure are the reference stress/strain curve ($a = 0$, $b = 0$) and the isothermal response ($a = 0$) corresponding to A (case B is similar).

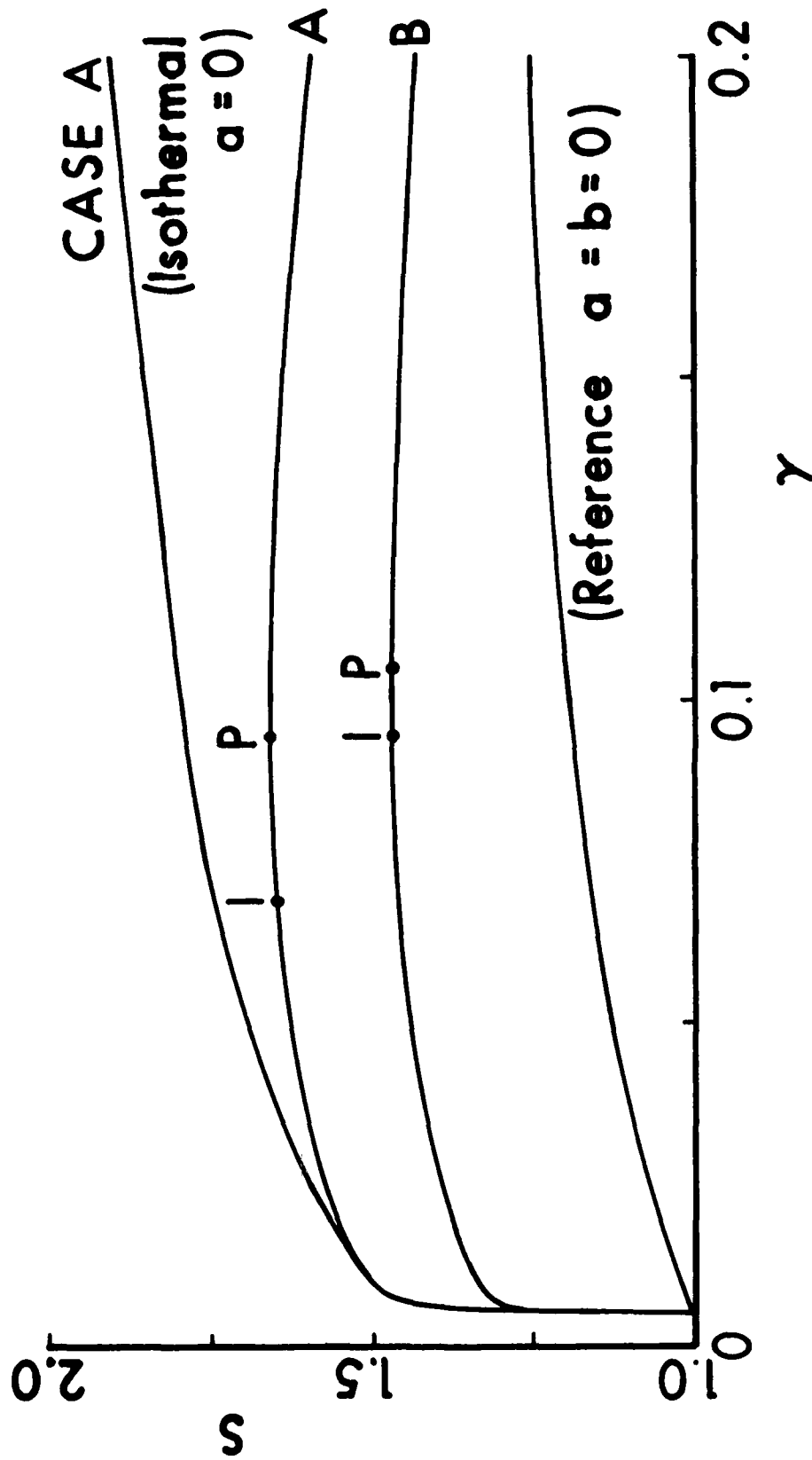


Figure 1. Homogeneous response curves. The reference curve, the isothermal curve for case A, and the adiabatic curves for both cases A and B are shown.

Perturbations to the homogeneous response have been introduced in the following manner. Just prior to the occurrence of peak stress, the temperature was modified by adding a symmetric bump at the center. Two cases have been considered as shown in Figure 2, the larger perturbation being five times higher and broader than the smaller one, but similar in shape. With the new temperature distribution given, the stress was recalculated so that $(2)_6$ is still satisfied, all other variables being held fixed. Then the full problem using all of (2) and the stated boundary conditions was restarted with the new field variables as initial data. After casting the equations into weak form, calculations were made using the finite element method, e.g. see Becker, et al.³

Case B with the smaller temperature bump as a perturbation was previously described in some detail in Reference 2. Figures 3 through 7 illustrate and compare the main features of the response for all cases considered to date. Because of the constant velocity maintained at the boundaries, average strain rate in the scaled variables for the strip $\dot{\gamma}_{ave}$ is exactly equal to one. This fact allows direct comparisons between the homogeneous and inhomogeneous cases. Figure 3 shows the stress at the center of the strip as a function of average strain (or time). The perturbation was added at the point marked I, and the peak of the homogeneous response is marked P. For the small temperature bump the stress follows the homogeneous response until well past the point P, and then drops rapidly as the shear band accelerates and localizes. The stress at other points of the strip is nearly the same, but lags slightly in time. Note that in real time (for $\dot{\gamma}_0 = 500 \text{ s}^{-1}$, say) the stress collapse is delayed approximately 125 μs past peak stress P, and the rapid acceleration itself takes more than 20 μs . This behavior is entirely similar for both cases A and B. The case of the larger temperature perturbation contrasts sharply. In this case the stress collapse begins even before point P.

Figures 4 and 5 show the evolution of temperature and plastic strain rate at the center and edge of the band in comparison to the homogeneous case. As is to be expected, the behavior parallels the stress response. At first the temperature and strain rate deviate slowly from the homogeneous response, but when the stress collapses, they both rise steeply in the center. At the edge, the temperature levels off to a plateau while the plastic strain rate (not shown for the edge position) drops towards zero. At first it appears that the temperature and plastic strain rate change so as to compensate each other without appreciably affecting the stress response, but eventually thermal softening wins out in the center. At the edge the stress drops due to momentum transfer from the center and effectively quenches both the temperature rise and the plastic deformation.

Figures 6 and 7 show cross sections of temperature and plastic strain rate for case A (with the larger temperature perturbation) at several times during the rapid transition. The most notable feature here is the narrowing of the most active region of deformation. This is particularly evident in the cross sections of plastic strain rate. Note that for the latest time the plastic strain rate in the center of the band is nearly 80 times the average applied strain rate.

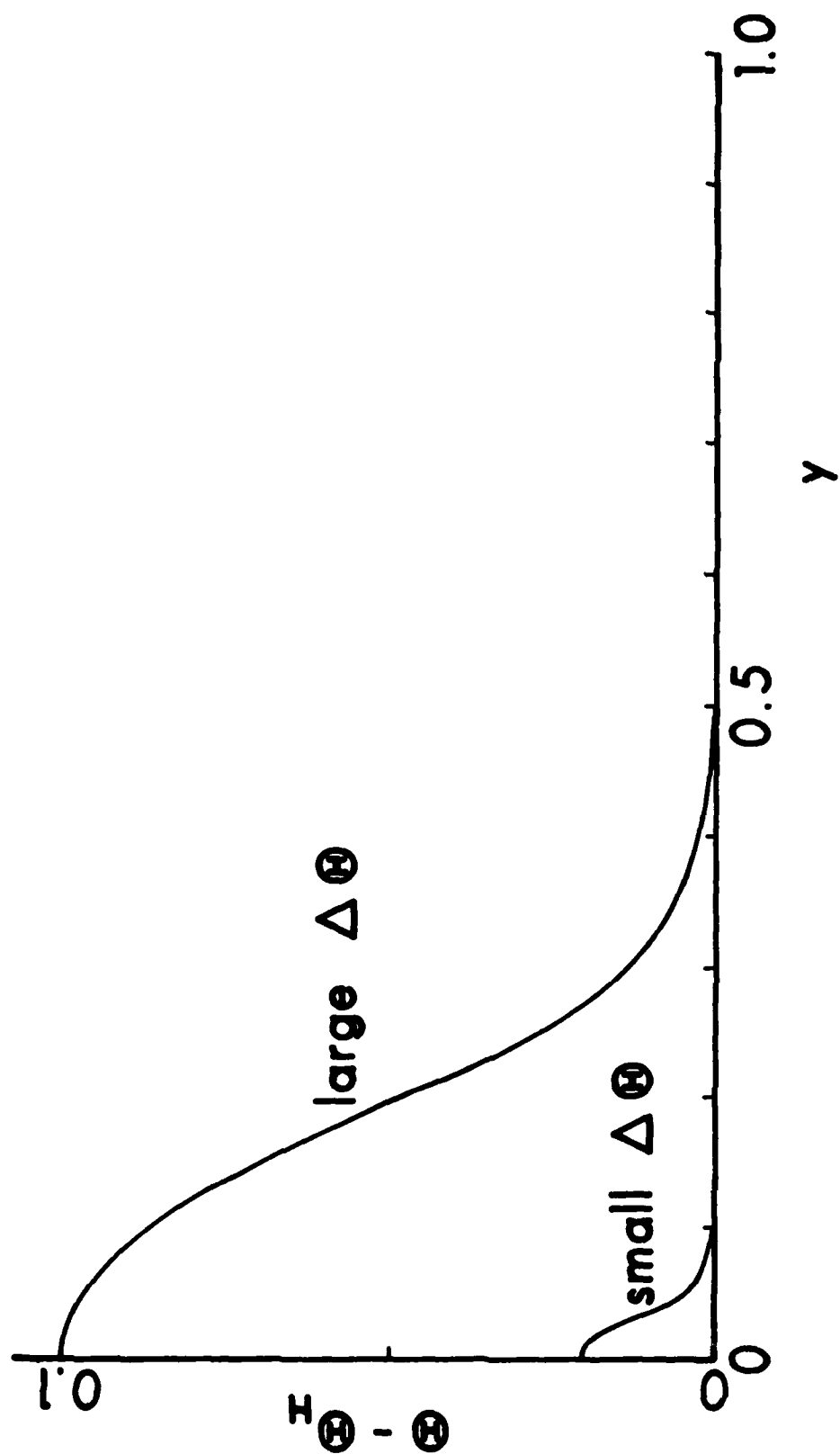


Figure 2. Temperature perturbations added to the homogeneous response at I.

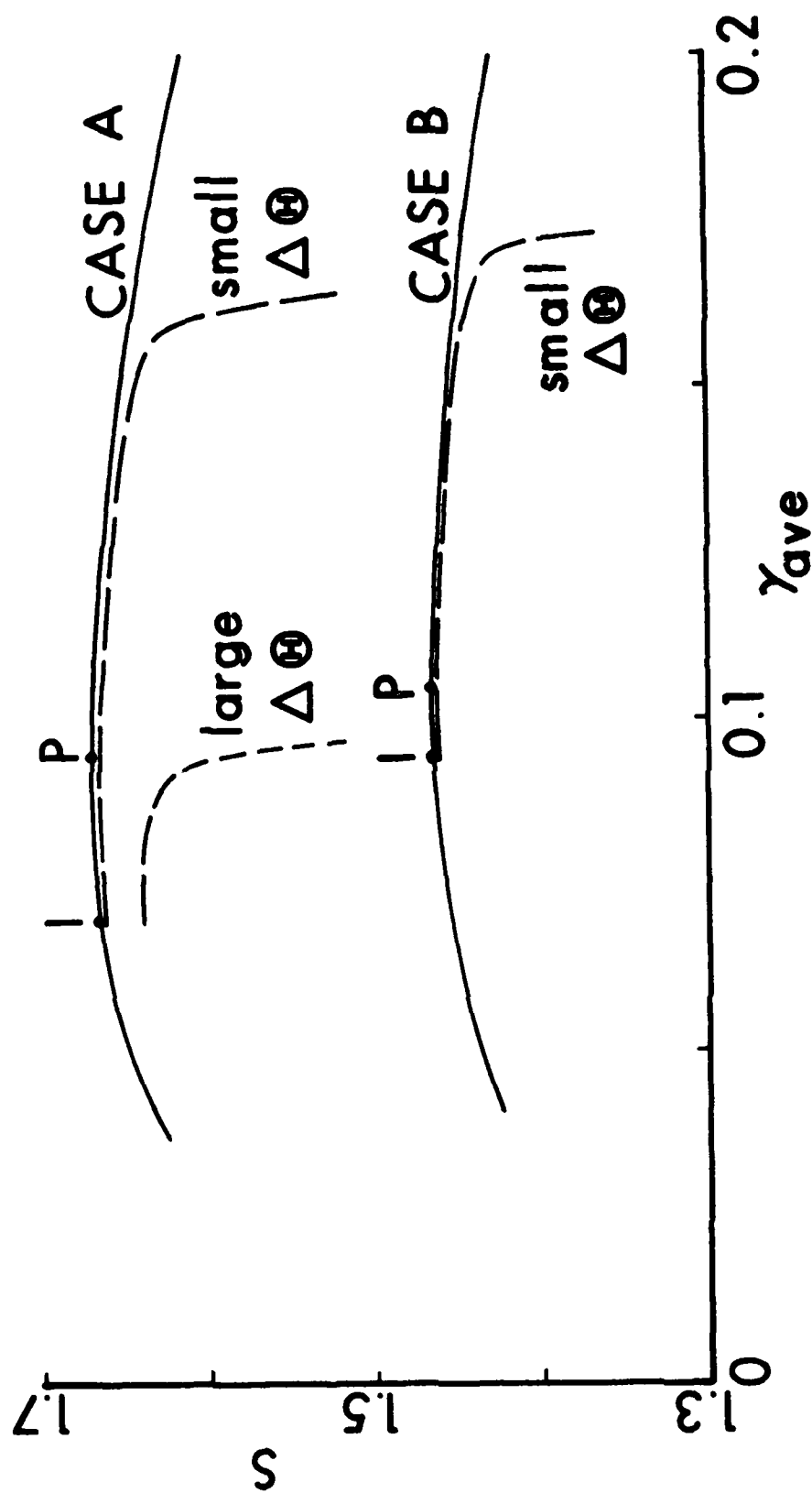


Figure 3. Stress vs. average strain (or time, since $\dot{\gamma}_{ave} = 1$). Homogeneous and perturbed responses for cases A and B.

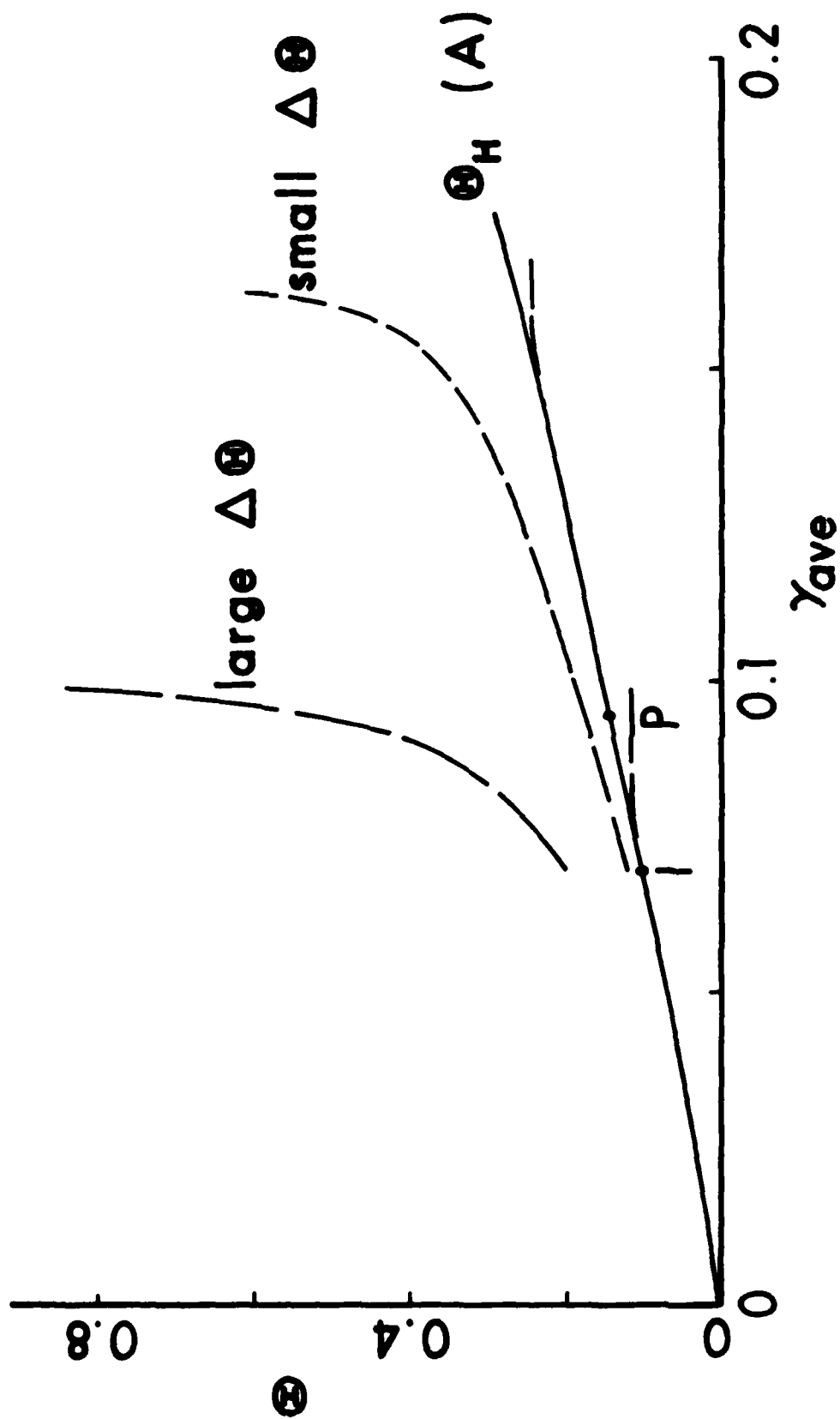


Figure 4. Temperature rise for case A. Upper curves are for the center of the band, lower curves for the edge. Solid curve is the homogeneous case.

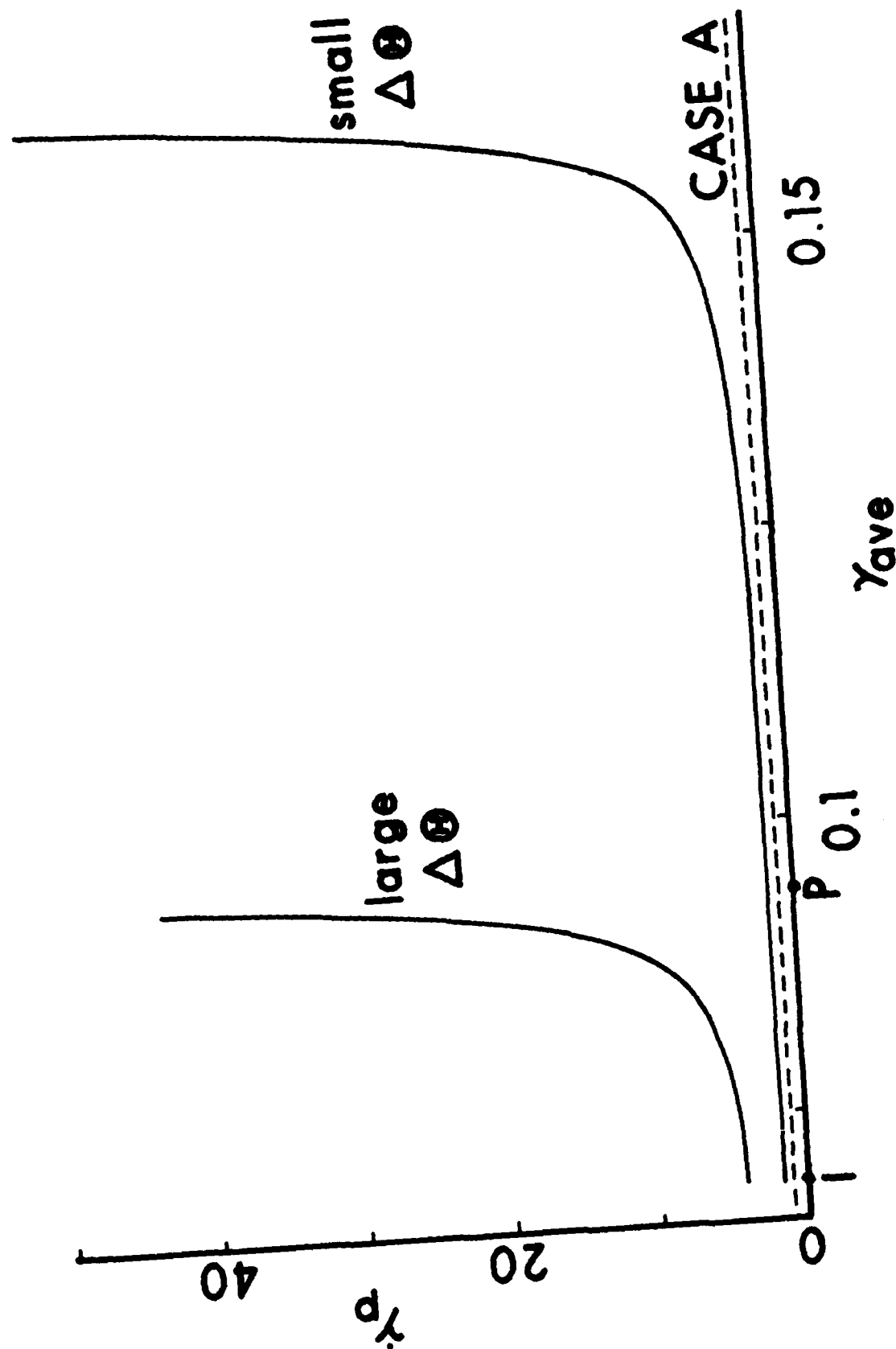


Figure 5. Plastic strain rate in the center of the band for case A. Reference rate (homogeneous deformation) is close to 1.

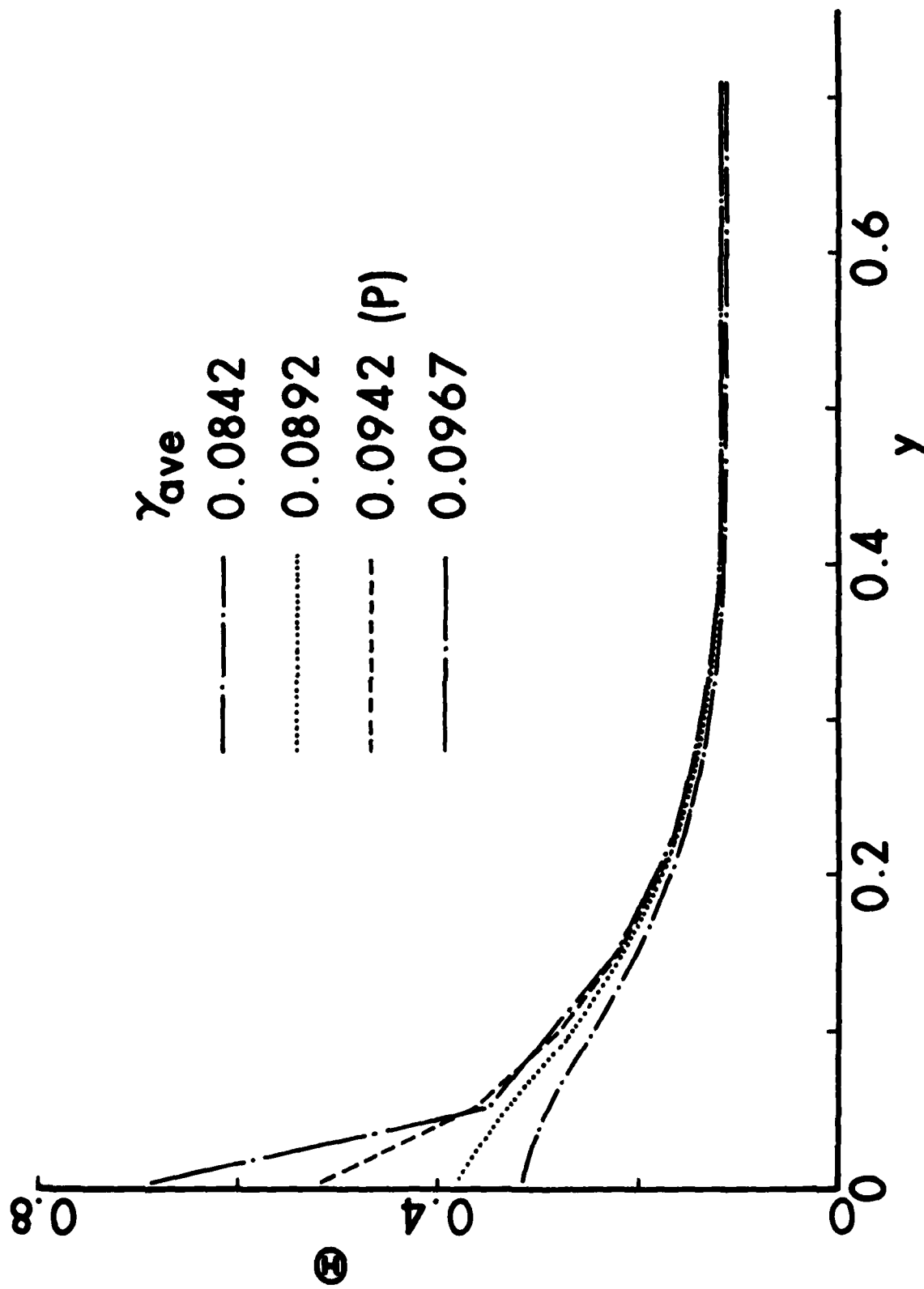


Figure 6. Cross sections of temperature rise at times indicated.

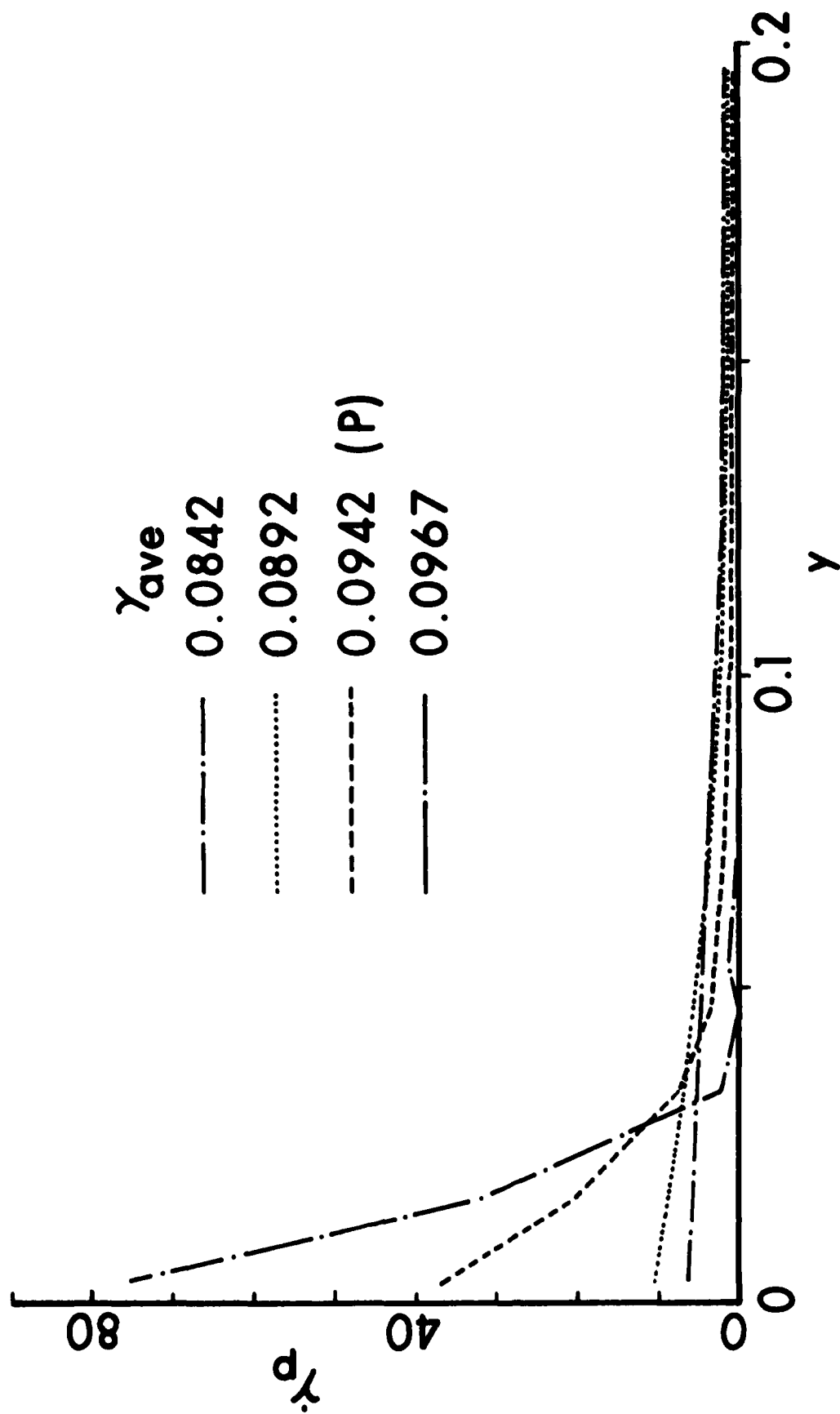


Figure 7. Cross sections of plastic strain rate at times indicated.

III. MODIFICATIONS FOR A DIPOLAR EFFECT

As a shear band forms, it is evident that very steep local strain gradients must develop. Therefore, it has seemed worthwhile to reformulate the problem in terms of a dipolar theory of plasticity. This has been accomplished in a straight forward manner by modifying the theory due to Green, McInnis, and Naghdi⁹ to include a rate effect. In a dipolar material it is assumed that, in addition to the usual traction forces that do work against velocities, there are hypertractions, denoted $\bar{\sigma}$ and having the dimensions of stress times length, that do work against velocity gradients. Decomposition of strain gradients into elastic and plastic parts introduces a new internal variable, denoted d_p in this paper, which requires its own evolutionary constitutive equation. As shown in Reference 9, dipolar plasticity introduces length scales that are characteristic of the material itself. In this paper, it is supposed that there is only one intrinsic length scale for elastic, plastic, or viscoplastic deformation, which is denoted $\bar{\ell}$. In addition to the nondimensional quantities introduced previously, we require

$$d_p = h \bar{d}_p, \quad \sigma = \bar{\sigma} / \bar{\ell} \kappa_0, \quad \ell = \bar{\ell} / h.$$

The full set of equations with a Von Mises type flow condition now takes the form

$$\text{Momentum: } (s - \ell \sigma, y), y = \rho \dot{v}$$

$$\text{Energy: } \dot{\theta} = k \theta, yy + s \dot{y}_p + \ell \sigma \dot{d}_p$$

Constitutive Equations:

$$\dot{s} = \mu (v, y - \dot{y}_p), \quad \dot{y}_p = \Lambda s$$

$$\dot{\sigma} = \ell \mu (v, yy - \dot{d}_p), \quad \dot{d}_p = \frac{\Lambda}{\ell} \sigma. \quad (3)$$

Reference Response and Work Hardening:

$$\kappa = (1 + \frac{\psi}{\psi_0})^n, \quad \dot{w}_p = \kappa \dot{\psi} = s \dot{y}_p + \ell \sigma \dot{d}_p$$

Yield condition:

$$(s^2 + \sigma^2)^{1/2} = (1 - a\theta)(1 + b\Lambda(s^2 + \sigma^2)^{1/2})^m \kappa.$$

In these equations Λ plays the role of a plastic multiplier and is to be determined from the yield condition when the loading point (s, σ, θ) lies outside the static yield surface, as determined by the last equation with Λ set equal to zero. Extra boundary conditions are also required. These are chosen to be $\sigma(+1, t) = 0$, so that the dipolar effect will effectively vanish outside the shear band.

Homogeneous solutions to these equations are exactly the same as before, but now the response to perturbations, computed for case B with the smaller temperature bump, appears to be quite different, although long computational run times have not yet been achieved. Figure 8 shows the evolution of the central plastic strain rate for a nondimensional intrinsic length $l = 10^{-2}$. The rate decays rapidly back toward the average applied rate, at least for short times after introduction of the perturbation, so that the dipolar effect appears to stabilize the deformation.

IV. DISCUSSION AND CONCLUSIONS

The response to the small temperature perturbation is qualitatively very similar for both cases A and B. Figure 3 shows that, although the stress levels are different due to the different viscous response, the shapes of the homogeneous response curves are similar, and so are the shapes of the response to perturbation. For something on the order of 5 or 6% average strain past the peak of the homogeneous curve the stress path deviates only slightly until stress collapse sets in at the end of the calculation. Similar behavior was reported by Merzer⁶ who used a completely different flow law for viscoplasticity. Thus, it appears that stress collapse is inherent in the process of band formation with the details depending on the specific material model used.

The calculation with the larger perturbation in temperature for case A shows that the details of stress collapse also depend strongly on the magnitude of the perturbation. Although case B has not been run with the larger temperature disturbance, there is no reason to expect that the results would be qualitatively different from case A.

The most striking aspect of the response patterns in Figure 3 is their similarity to those obtained in analyzing imperfection sensitivity for a bifurcation problem, e.g., see Reference 10. The only thing missing is the bifurcation branch itself. Figures 4 and 5 for temperature and plastic strain rate reinforce this idea.

Although calculations for the dipolar case have not yet progressed far enough to be definitive, it appears that the effect, even for a very small inherent material length scale, will be highly stabilizing. This would be in accordance with the experience to date for elastic systems where, as in Reference 11, higher order effects allow smooth transitions instead of discontinuities.

Unfortunately, because of computational instabilities that set in, it has not yet been possible to continue calculations to the point where a final configuration for the shear band appears. The calculations reported in Reference 2 indicated that a peak value for plastic strain rate may occur, but reexamination has indicated numerical instability. The difficulty seems to be that eventually the extreme localization of the band defeats the ability of the present numerical method to resolve the details.

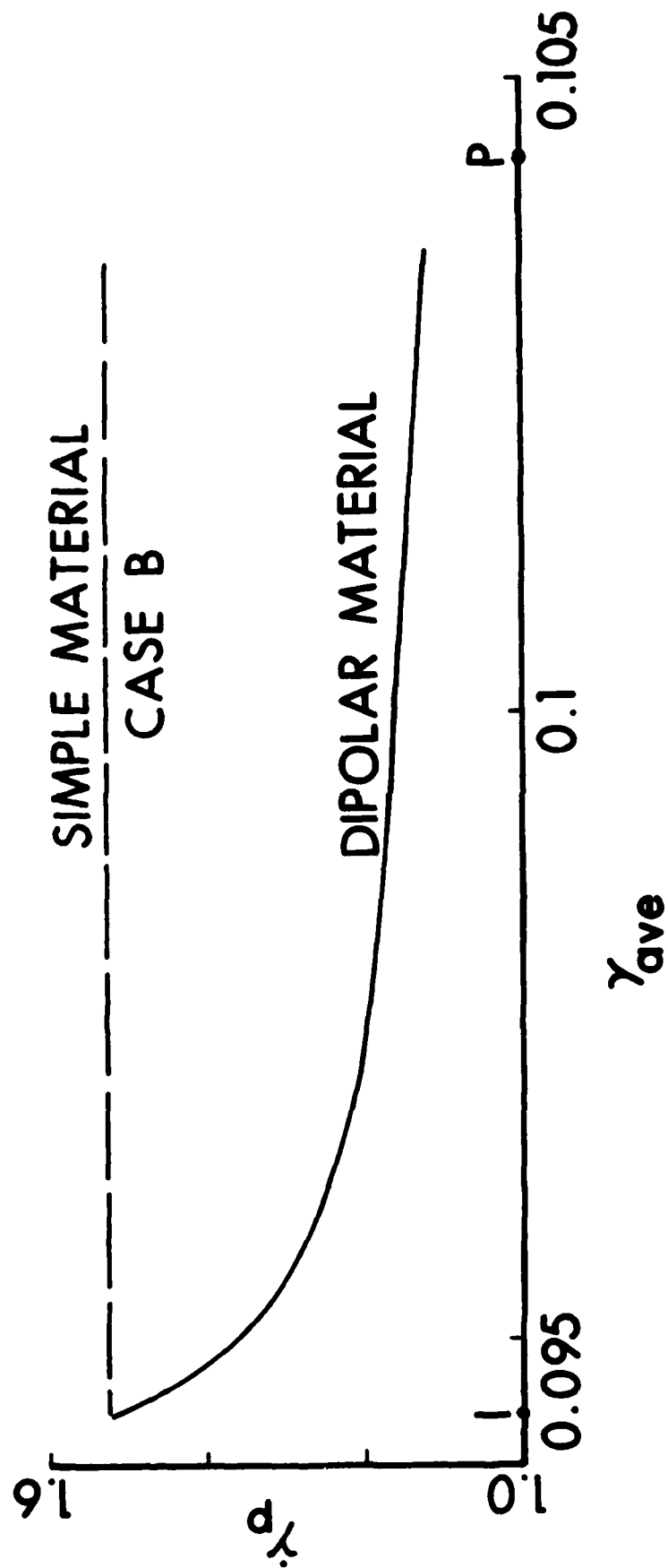


Figure 8. Plastic strain rate in the center of the band for case B at early times. Dipolar material compared to simple material.

REFERENCES

1. R. J. Clifton, J. Duffy, K. A. Hartley, and T. G. Shawki, *Scrip. Met.* 18 (1984) 443.
2. T. W. Wright and R. C. Batra, *Int. J. Plas.* 1 (1985) in press.
3. J. Litonski, *Bull. l'Acad. Pol. Sci.* 25 (1977) 7.
4. G. R. Johnson, J. M. Hoegfelt, U. S. Lindholm, and A. Nagy, *J. Eng. Mat. & Tech., Trans. ASME* 105 (1983) 42 and 105 (1983) 48.
5. T. J. Burns, Sandia Report SAND83-1901, Albuquerque, NM (1983).
6. A. M. Merzer, *J. Mech. Phys. Sol.* 30 (1982) 323.
7. L. S. Costin, E. E. Crisman, R. H. Hawley, and J. Duffy, in Mechanical Properties at High Rates of Strain, 1979, *Inst. Phys.* 47 (1979) 90.
8. E. B. Becker, G. F. Carey, and J. T. Oden, Finite Elements, An Introduction, Prentice-Hall (1981) Englewood Cliffs, NJ.
9. A. E. Green, B. C. McInnis, and P. M. Naghdi, *Int. J. Eng. Sci.* 6 (1968) 373.
10. G. Iooss, and D. D. Joseph, Elementary Stability and Bifurcation Theory, Springer-Verlag (1980) New York - Heidelberg-Berlin.
11. E. C. Aifantis, and J. C. Serrin, *J. Colloid and Interface Sci.* 96 (1983) 517 and 96 (1983) 530.

DISTRIBUTION LIST

<u>No. of Copies</u>	<u>Organization</u>	<u>No. of Copies</u>	<u>Organization</u>
12	Administrator Defense Technical Info Center ATTN: DDC-DDA Cameron Station Alexandria, VA 22304-6145	4	Commander Armament R&D Center US Army AMCCOM ATTN: SMCAR-SC, J. D. Corrie J. Beetle E. Bloore P. Harris Dover, NJ 07801
2	Director Defense Advanced Research Projects Agency ATTN: Tech Info Dr. E. Van Reuth 1400 Wilson Boulevard Arlington, VA 22209	1	Commander Armament R&D Center US Army AMCCOM ATTN: SMCAR-TDC Dover, NJ 07801
1	Deputy Assistant Secretary of the Army (R&D) Department of the Army Washington, DC 20310	1	Commander Armament R&D Center US Army AMCCOM ATTN: SMCAR-TSS Dover, NJ 07801
1	HQDA DAMA-ART-M Washington, DC 20310	1	Commander Benet Weapons Laboratory ATTN: Dr. E. Schneider Watervliet, NY 12189
1	Commander US Army War College ATTN: Lib Carlisle Barraacks, PA 17013	1	Director Benet Weapons Laboratory Armament R&D Center US Army AMCCOM ATTN: SMCAR-LCB-TL Watervliet, NY 12189
1	Commander US Army Command and General Staff College ATTN: Archives Fort Leavenworth, KS 66027	1	Commander US Army Armament, Munitions and Chemical Command ATTN: SMCAR-ESP-L Rock Island, IL 61299
1	Commander US Army Materiel Command ATTN: AMCDRA-ST 5001 Eisenhower Avenue Alexandria, VA 22333-0001	1	Commander US Army Aviation Research and Development Command ATTN: AMSAV-E 4300 Goodfellow Boulevard St. Louis, MO 63120

DISTRIBUTION LIST

<u>No. of Copies</u>	<u>Organization</u>	<u>No. of Copies</u>	<u>Organization</u>
1	Director US Army Air Mobility Research and Development Command Ames Research Center Moffett Field, CA 94035	2	Commander US Army Mobility Equipment Research & Development Command ATTN: DRDME-WC DRSME-RZT Fort Belvoir, VA 22060
1	Commander US Army Communications - Electronics Command ATTN: AMSEL-ED Fort Monmouth, NJ 07703-5301	1	Commander US Army Natick Research and Development Center ATTN: DRXRE, Dr. D. Sieling Natick, MA 01762
1	Commander ERADCOM Technical Library ATTN: DELSD-L (Reports Section) Fort Monmouth, NJ 07703-5301	1	Commander US Army Tank Automotive Command ATTN: AMSTA-TSL Warren, MI 48397-5000
1	Commander US Army Harry Diamond Laboratory ATTN: DELHD-TA-L 2800 Powder Mill Road Adelphi, MD 20783	1	Commander US Army Electronics Proving Ground ATTN: Tech Lib Fort Huachuca, AZ 85613
1	Commander MICOM Research, Development and Engineering Center ATTN: AMSMI-RD Redstone Arsenal, AL 35898-5500	1	Commander US Army Development and Employment Agency ATTN: MODE-TED-SAB Fort Lewis, WA 98433
1	Director Missile and Space Intelligence Center ATTN: AIAMS-YDL Redstone Arsenal, AL 35898-5500	3	Commander US Army Materials and Mechanics Research Center ATTN: AMXMR-T, J. Mescall AMXMR-T, R. Shea AMXMR-H, S.C. Chou Watertown, MA 02172
3	Director BMD Advanced Technology Center ATTN: ATC-T, M. Capps ATC-M, S. Brockway ATC-RN, P. Boyd P.O. Box 1500 Huntsville, AL 35807	1	Director US Army TRADOC Systems Analysis Activity ATTN: ATAA-SL White Sands Missile Range, 88002

DISTRIBUTION LIST

<u>No. of</u> <u>Copies</u>	<u>Organization</u>	<u>No. of</u> <u>Copies</u>	<u>Organization</u>
1	Commandant US Army Infantry School ATTN: ATSH-CD-CSO-OR Fort Benning, GA 31905	3	Commander Naval Surface Weapons Center ATTN: Dr. W. H. Holt Dr. W. Mock Tech Lib Dahlgren, VA 22448
1	Director US Army Advanced BMD Technology Center ATTN: CRDABH-5, W. Loomis P. O. Box 1500, West Station Huntsville, AL 35807	3	Commander Naval Surface Weapons Center ATTN: Dr. R. Crowe Code R32, Dr. S. Fishman Tech Lib Silver Spring, MD 20910
3	Commander US Army Research Office ATTN: Dr. E. Saibel Dr. G. Mayer Dr. J. Chandra P. O. Box 12211 Research Triangle Park, NC 27709	1	Commander and Director US Naval Electronics Laboratory San Diego, CA 92152
2	Commander US Army Research and Standardization Group (Europe) ATTN: Dr. J. Wu Dr. F. Oertel Box 65 FPO NY 09510	5	Air Force Armament Laboratory ATTN: AFATL/DLODL J. Foster John Collins Joe Smith Guy Spitale Eglin AFB, FL 32542-5000
2	Office of Naval Research Department of the Navy ATTN: Code 402 Washington, DC 20360	1	RADC (EMTLD, Lib) Griffiss AFB, NY 13440
3	Commander US Naval Air Systems Command ATTN: AIR-604 Washington, DC 20360	1	AFWL/SUL Kirtland AFB, NM 87117
1	Commander Naval Ordnance Systems Command Washington, DC 20360	1	AUL (3T-AUL-60-118) Maxwell AFB, AL 36112
		2	Air Force Wright Aeronautical Laboratories Air Force Systems Command Materials Laboratory ATTN: Dr. Theodore Nicholas Dr. John P. Henderson Wright-Patterson AFB, OH 45433

DISTRIBUTION LIST

<u>No. of Copies</u>	<u>Organization</u>	<u>No. of Copies</u>	<u>Organization</u>
1	Director Environmental Science Service Administration US Department of Commerce Boulder, CO 80302	1	Forestal Research Center Aeronautical Engineering Lab. Princeton University ATTN: Dr. A. Eringen Princeton, NJ 08540
1	Director Lawrence Livermore Laboratory ATTN: Dr. M. L. Wilkins P. O. Box 808 Livermore, CA 94550	1	Honeywell, Inc. Defense Systems Division ATTN: Dr. Gordon Johnson 600 Second street, NE Hopkins, MN 55343
8	Sandia National Laboratories ATTN: Dr. L. Davison Dr. P. Chen Dr. L. Bertholf Dr. W. Herrmann Dr. J. Nunziato Dr. S. Passman Dr. E. Dunn Dr. T. Burns Dr. M. Forrestal Albuquerque, NM 87115	1	IBM Watson Research Center ATTN: R. A. Toupin Poughkeepsie, NY 12601
1	Director National Aeronautics and Space Administration Lyndon B. Johnson Space Center ATTN: Lib Houston, TX 77058	2	Orlando Technology, Inc. ATTN: Dr. Daniel Matuska Dr. John J. Osborn P. O. Box 855 Shalimar, FL 32579
1	Director Jet Propulsion Laboratory ATTN: Lib (TDS) 4800 Oak Grove Drive Pasadena, CA 91103	6	SRI International ATTN: Dr. Donald R. Curran Dr. Donald A. Shockey Dr. Lynn Seaman Mr. D. Erlich Dr. A. Florence Dr. R. Caligiuri 333 Ravenswood Avenue Menlo Park, CA 94025
1	Aeronautical Research Associates of Princeton, Incorporated ATTN: Ray Gogolewski 1800 Old Meadow Rd., #114 McLean, VA 22102	1	Systems Planning Corporation ATTN: Mr. T. Hafer 1500 Wilson Boulevard Arlington, VA 22209
		1	Terra-Tek, Inc. ATTN: Dr. Arfon Jones 420 Wahara Way University Research Park Salk Lake City, UT 84108

DISTRIBUTION LIST

<u>No. of Copies</u>	<u>Organization</u>	<u>No. of Copies</u>	<u>Organization</u>
2	California Institute of Technology Division of Engineering and Applied Science ATTN: Dr. E. Sternberg Dr. J. Knowles Pasadena, CA 91102	1	Brown University Division of Applied Mathematics ATTN: Prof. C. Dafermos Providence, ri 02912
1	Denver Research Institute University of Denver ATTN: Dr. R. Recht P. O. Box 10127 Denver, CO 80210	3	Carnegie-Mellon University Department of Mathematics ATTN: Dr. D. Owen Dr. M. E. Gurtin Dr. B. D. Coleman Pittsburgh, PA 15213
1	Massachusetts Institute of Technology ATTN: Dr. R. Probststein 77 Massachusetts Avenue Cambridge, MA 02139	7	Cornell University Department of Theoretical and Applied Mechanics ATTN: Dr. Y. H. Pao Dr. G. S. S. Ludford Dr. A. Ruoff Dr. J. Jenkins Dr. R. Lance Dr. F. Moon Dr. E. Hart Ithaca, NY 14850
3	Rensselaer Polytechnic Institute ATTN: Prof. E. H. Lee Prof. E. Krempl Prof. J. Flaherty Troy, NY 12181	1	Harvard University Division of Engineering and Applied Physics ATTN: Prof. J. R. Rice Prof. J. Hutchinson Cambridge, MA 02138
2	Southwest Research Institute Department of Mechanical Sciences ATTN: Dr. U. Lindholm Dr. W. Baker 8500 Culebra Road San Antonio, TX 78228	1	Iowa State University Engineering Research Laboratory ATTN: Dr. A. Sedov Dr. G. Nariboli Ames, IA 50010
5	Brown University Division of Engineering ATTN: Prof. R. Clifton Prof. H. Kolsky Prof. L. B. Freund Prof. A. Needleman Prof. R. Asaro Providence, RI 02912	2	Lehigh University Center for the Application of Mathematics ATTN: Dr. E. Varley Dr. R. Rivlin Bethlehem, PA 18015

DISTRIBUTION LIST

<u>No. of Copies</u>	<u>Organization</u>	<u>No. of Copies</u>	<u>Organization</u>
1	New York University Department of Mathematics ATTN: Dr. J. Keller University Heights New York, NY 10053	1	Tulane University Department of Mechanical Engineering ATTN: Dr. S. Cowin New Orleans, LA 70112
1	North Carolina State University Department of Civil Engineering ATTN: Prof. Y. Horie Raleigh, NC 27607	3	University of California Department of Mechanical Engineering ATTN: Dr. M. Carroll Dr. W. Goldsmith Dr. P. Naghdi Berkeley, CA 94704
1	Pennsylvania State University Engineering Mechanical Dept. ATTN: Prof. N. Davids University Park, PA 16502	1	University of California Dept of Aerospace and Mechanical Engineering Science ATTN: Dr. Y. C. Fung P. O. Box 109 La Jolla, CA 92037
1	Rice University ATTN: Dr. C. C. Wang P. O. Box 1892 Houston, TX 77001	1	University of California Department of Mechanics ATTN: Dr. R. Stern 504 Hilgard Avenue Los Angeles, CA 90024
1	Southern Methodist University Solid Mechanics Division ATTN: Prof. H. Watson Dallas, TX 75221	1	University of California at Santa Barbara Department of Mechanical Engineering ATTN: Prof. T. P. Mitchel Santa Barbara, CA 93106
1	Temple University College of Engineering Tech. ATTN: Dr. R. Haythornthwaite Dean Philadelphia, PA 19122	2	University of Delaware Department of Mechanical and Aerospace Engineering ATTN: Dr. Minoru Taya Prof. J. Vinson Newark, DE 19711
5	The Johns Hopkins University ATTN: Prof. R. B. Pond, Sr. Prof. R. Green Prof. W. Sharpe Prof. J. F. Bell Prof. C. A. Truesdell 34th and Charles Streets Baltimore, MD 21218		

DISTRIBUTION LIST

<u>No. of Copies</u>	<u>Organization</u>	<u>No. of Copies</u>	<u>Organization</u>
3	University of Florida Department of Engineering Science and Mechanics ATTN: Prof. L. Malvern Prof. D. Drucker Prof. E. Walsh Gainesville, FL 32601	2	University of Maryland Department of Mathematics ATTN: Prof. S. Antman Prof. T. P. Liu College Park, MD 20742
2	University of Houston Department of Mechanical Engineering ATTN: Dr. T. Wheeler Dr. R. Nachlinger Houston, TX 77004	3	University of Minnesota Department of Engineering Mechanics ATTN: Prof. J. L. Erickson Prof. R. Fosdick Prof. R. James Minneapolis, MN 55455
1	University of Illinois Department of Theoretical and Applied Mechanics ATTN: Dr. D. Carlson Urbana, IL 61801	1	University of Pennsylvania Towne School of Civil and Mechanical Engineering ATTN: Prof. Z. Hashin Philadelphia, PA 19105
2	University of Illinois at Chicago Circle College of Engineering Department of Engineering, Mechanics, and Metallurgy ATTN: Prof. T.C.T. Ting Prof. D. Krajcinovic P. O. Box 4348 Chicago, IL 60680	4	University of Texas Department of Engineering Mechanics ATTN: Dr. M. Stern Dr. M. Bedford Prof. Ripperger Dr. J. T. Oden Austin, TX 78712
2	University of Kentucky Department of Engineering Mechanics ATTN: Dr. M. Beatty Prof. O. Dillon, Jr. Lexington, KY 40506	1	University of Washington Department of Aeronautics and Astronautics ATTN: Dr. Ian M. Fyfe 206 Guggenheim Hall Seattle, WA 98195
1	University of Kentucky School of Engineering ATTN: Dean R. M. Bowen Lexington, KY 40506	3	Washington State University Department of Physics ATTN: Prof. R. Fowles Prof. G. Duvall Prof. Y. Gupta Pullman, WA 99163

DISTRIBUTION LIST

<u>No. of Copies</u>	<u>Organization</u>	<u>No. of Copies</u>	<u>Organization</u>
2	Yale University ATTN: Dr. B.-T. Chu Dr. E. Onat 400 Temple Street New Haven, CT 96520	10	Central Intelligence Agency Office of Central Reference Dissemination Branch Room GE-47 HQS Washington, D.C. 20502

Aberdeen Proving Ground

Dir, USAMSAA
ATTN: AMXSY-D
AMXSY-MP, H. Cohen
Cdr, USATECOM
ATTN: AMSTE-TO-F
Cdr, CRDC, AMCCOM
ATTN: SMCCR-RSP-A
SMCCR-MU
SMCCR-SPS-IL

USER EVALUATION SHEET/CHANGE OF ADDRESS

This Laboratory undertakes a continuing effort to improve the quality of the reports it publishes. Your comments/answers to the items/questions below will aid us in our efforts.

1. BRL Report Number _____ Date of Report _____
2. Date Report Received _____
3. Does this report satisfy a need? (Comment on purpose, related project, or other area of interest for which the report will be used.) _____

4. How specifically, is the report being used? (Information source, design data, procedure, source of ideas, etc.) _____

5. Has the information in this report led to any quantitative savings as far as man-hours or dollars saved, operating costs avoided or efficiencies achieved, etc? If so, please elaborate. _____

6. General Comments. What do you think should be changed to improve future reports? (Indicate changes to organization, technical content, format, etc.) _____

CURRENT ADDRESS	_____
	Name

	Organization

	Address

	City, State, Zip

7. If indicating a Change of Address or Address Correction, please provide the New or Correct Address in Block 6 above and the Old or Incorrect address below.

OLD ADDRESS	_____
	Name

	Organization

	Address

	City, State, Zip

(Remove this sheet along the perforation, fold as indicated, staple or tape closed, and mail.)

----- FOLD HERE -----

Director
U.S. Army Ballistic Research Laboratory
ATTN: SLCBR-DD-T
Aberdeen Proving Ground, MD 21005-5066

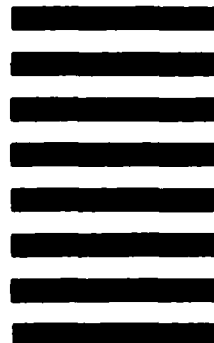


NO POSTAGE
NECESSARY
IF MAILED
IN THE
UNITED STATES

OFFICIAL BUSINESS
PENALTY FOR PRIVATE USE, \$300

BUSINESS REPLY MAIL
FIRST CLASS PERMIT NO 12062 WASHINGTON, DC
POSTAGE WILL BE PAID BY DEPARTMENT OF THE ARMY

Director
U.S. Army Ballistic Research Laboratory
ATTN: SLCBR-DD-T
Aberdeen Proving Ground, MD 21005-9989



----- FOLD HERE -----

END

DTIC

6-86